UNIVERSITY OF BIRMINGHAM
University of Birmingham Research at Birmingham

Conductivity measurement using 3D printed re-entrant cavity resonator

Mohammed, Ali Musa; Wang, Yi; Skaik, Talal; Li, Sheng; Attallah, Moataz

DOI:
10.1088/1361-6501/ac5134

License:
Creative Commons: Attribution (CC BY)

Document Version
Publisher's PDF, also known as Version of record

Citation for published version (Harvard):
Mohammed, AM, Wang, Y, Skaik, T, Li, S & Attallah, M 2022, 'Conductivity measurement using 3D printed re-entrant cavity resonator', *Measurement Science and Technology*, vol. 33, no. 5, 055017. https://doi.org/10.1088/1361-6501/ac5134

Link to publication on Research at Birmingham portal

General rights
Unless a licence is specified above, all rights (including copyright and moral rights) in this document are retained by the authors and/or the copyright holders. The express permission of the copyright holder must be obtained for any use of this material other than for purposes permitted by law.

•Users may freely distribute the URL that is used to identify this publication.
•Users may download and/or print one copy of the publication from the University of Birmingham research portal for the purpose of private study or non-commercial research.
•User may use extracts from the document in line with the concept of 'fair dealing' under the Copyright, Designs and Patents Act 1988 (?)
•Users may not further distribute the material nor use it for the purposes of commercial gain.

Where a licence is displayed above, please note the terms and conditions of the licence govern your use of this document.

When citing, please reference the published version.

Take down policy
While the University of Birmingham exercises care and attention in making items available there are rare occasions when an item has been uploaded in error or has been deemed to be commercially or otherwise sensitive.

If you believe that this is the case for this document, please contact UBIRA@lists.bham.ac.uk providing details and we will remove access to the work immediately and investigate.

Download date: 24. Apr. 2024

PAPER • **OPEN ACCESS**

Conductivity measurement using 3D printed re-entrant cavity resonator

To cite this article: Ali Musa Mohammed *et al* 2022 *Meas. Sci. Technol.* **33** 055017

View the article online for updates and enhancements.

You may also like

- An investigation on microstructure and mechanical behaviour of copper-nickel coated carbon fibre reinforced aluminium composites
K Gajalakshmi, N Senthilkumar, B Mohan et al.
- Effect of stir cast process parameters on wear behaviour of copper coated short steel fibers reinforced LM13 aluminium alloy composites
Samson Jerold Samuel Chelladurai and Ramesh Arthanari
- Influence of Glycerol on Copper Electrodeposition from Pyrophosphate Bath: Nucleation Mechanism and Performance Characterization
Jiaping Hu, Qingyang Li, Maozhong An et al.

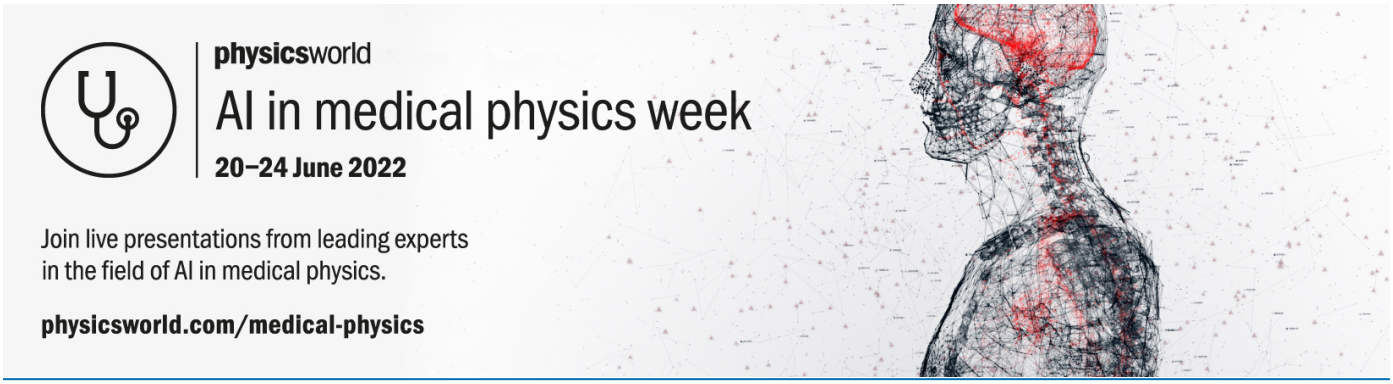

This content was downloaded from IP address 147.188.216.50 on 16/06/2022 at 16:16

OPEN ACCESS
IOP Publishing
Measurement Science and Technology
Meas. Sci. Technol. **33** (2022) 055017 (7pp)
https://doi.org/10.1088/1361-6501/ac5134

Conductivity measurement using 3D printed re-entrant cavity resonator

Ali Musa Mohammed[1,2,*], **Yi Wang**[1], **Talal Skaik**[1], **Sheng Li**[3] **and Moataz Attallah**[3]

[1] School of Electronic, Electrical and Systems Engineering, University of Birmingham, Birmingham, United Kingdom
[2] The Federal Polytechnic Damaturu, Yobe, Nigeria
[3] School of Metallurgy and Materials University of Birmingham, Birmingham B15 2TT, United Kingdom

E-mail: alimusa@fedpodam.edu.ng and amm338@bham.ac.uk

Received 18 November 2021, revised 18 January 2022
Accepted for publication 2 February 2022
Published 18 February 2022

Abstract

A technique for measuring effective conductivity of conductor materials using 3D printed re-entrant cavity resonator is proposed. An analytical formula for the extraction of the effective conductivity has been derived in relation to energy stored in the volume of the cavity geometry. A method of resonant cavity characterisation of material based on microwave losses is utilised for the measurements. The approach offers a simplified analytical method and also supports the measurements of sample with arbitrary thickness. Samples produced from three different manufacturing processes of computer numerical control (CNC) and 3D printing, made of aluminium, copper and stainless steel were measured to demonstrate the method. The 3D printed and copper coated polymer sample is considered as reference material for the measurements. The measured results have shown that the copper coated polymer sample have similar conductivity with that CNC copper. This signifies the good finishing, low surface roughness and quality of copper coating used in 3D printed polymer device.

Keywords: additive manufacturing, conductivity, 3D printing, re-entrant cavity, surface roughness

(Some figures may appear in colour only in the online journal)

1. Introduction

Additive manufacturing (AM) has been utilised in fabrication of microwave devices such as cavity based resonator sensors, filters and antennas [1–5]. The technology has been used in producing structures of complex nature in separate parts or in a monolithic form giving them advantage over other fabrication methods [2]. For example: a 3D printed polymer sensor made using stereolithographic apparatus (SLA) process and coated with copper was presented in [3]. Other examples include a 3D printed metallic filter fabricated by micro laser sintering [4] and 3D printed horn antennas [5]. Therefore, 3D printing technology offers various opportunities in terms of materials, cost reduction and realisation of complex structures that are effective for microwave design. Structures that cannot be machined easily using a conventional means (e.g. computer numerical control (CNC) milling) can be realised at low cost. However, the performance of these 3D printed microwave devices greatly depends on the losses associated with the metallic surface or metallic coating. Accurate evaluation of effective conductivity or surface resistance of the conductors at microwave frequencies are highly important for the modelling of these devices and predicting their performance. In principle, the loss characteristics of these structures can be computed theoretically based on analytical models with assumptions about the dc bulk conductivity and an ideally smooth wall [6]. However, in practice the situation is different as this assumption cannot account for the effect of metallic surface quality (surface roughness, morphology, and composition) that may produce

* Author to whom any correspondence should be addressed.

Original content from this work may be used under the terms of the Creative Commons Attribution 4.0 licence. Any further distribution of this work must maintain attribution to the author(s) and the title of the work, journal citation and DOI.

 © 2022 The Author(s). Published by IOP Publishing Ltd

excess losses. For this, microwave measurement techniques for the characterisation of effective conductivity of materials have been extensively studied and reported in literature [7–11]. Two major techniques were adopted for decades: non-resonant method (such as the transmission line based) and resonant method. Both techniques have been explained in detail in [7]. The resonant method is considered to provide results that are more accurate and precise due to the high Q-factor of the resonators [12]. The resonant method technique has the advantage that the losses within the cavity at the desired resonance frequency are sensitive to the changes in the conductivity of the material. This is in contrast to the transmission line techniques, where the conductor losses are often small, and resolving the conductivity becomes difficult. However, the transmission line method supports a broad range of frequencies while the resonant method is limited to discrete frequencies [13].

In [14], measurement of dc conductivity of highly conductive polyaniline films has been reported using three different methods at different frequencies. These include: resonant, surface impedance and transmission line techniques. In the resonant cavity technique, the sample was placed in the centre of the cavity where magnetic field is maximum to measure the changes due to material insertion and used the Q-factor to evaluate the conductivity of the materials. Results from all the methods were compared with value reported in literature. The resonant techniques offer the highest accuracy with uncertainty mainly determined by sample placements [14]. Conductivity measurements of doped semiconductors materials have also been demonstrated [15]. The finding shows superlinear power law of frequency dependency of the conductivity. Similarly, a linear temperature dependence of copper resistivity has been reported using a novel toroid split-ring resonator [16].

A recent work has reported an estimation of the surface resistance of materials for microwave applications based on Fabry–Perot open resonator over the range of 20–40 GHz [17]. The high Q-factor of the resonator allows measurements up to a conductivity with a magnitude of 10^4 S m^{-1}. The results agree with the expected values of materials under test (MUT). However, there is about 30% difference between the measured and the expected values. On the other hand, due to effect of vibrations and spectral variation of coupling level associated with this technique and the measurement set-up, materials with low conductivity can be greatly affected, leading to large error. In [18] an investigation into aluminium-silicon-magnesium alloy for microwave devices via conductivity measurement is reported. Simple rectangular waveguide cavity structures were used. The study focuses on the large-scale geometry variation from the materials rather than the surface roughness. The measured average conductivity of the cavities from two manufacturers shows about 70% difference from nominal conductivity of the aluminium alloy. The measured value was used in the simulation and result agrees well with the measurement. This has therefore validated the results of the measured conductivity of the materials under investigation [18].

More recently a study for an alternative test fixture for evaluating and distinguishing various materials through their electric resistance has been detailed in [19]. In this work, a new measurement approach is described using a re-entrant cavity resonator. The end wall replacements method similar to [20] is adopted. A simplified analytical formula is developed based on the energy stored in the cavity and simulations. This is different from [11] which used a more complex expression of the ohmic Q-factor associated with the mode of interest and the cavity geometry.

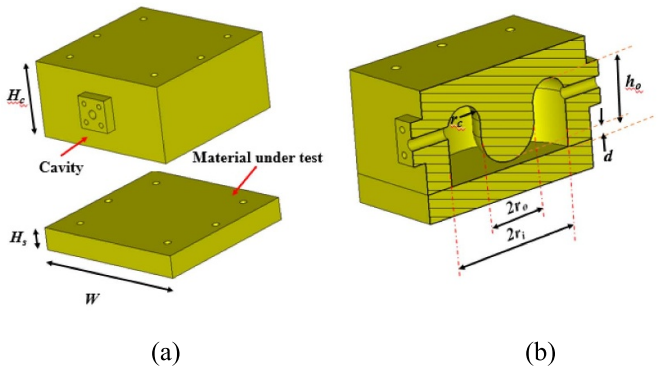

Figure 1. Re-entrant cavity resonator (a) 3D model of cavity and MUT $Hc = 35.45$ mm, $Hs = 10$ mm, $W = 70$ mm and (b) inner view and assembled cavity.

Section 2 of the paper describes the design of the cavity. The measurement method and results of the measured resonance frequency and Q-factors of all the samples is given in section 3. Sections 4 discuss surface roughness and its measurements for all the samples made using different technologies. The simplified method for the extraction of the effective conductivity of measured materials has been derived in section 5. The results are fully discussed in section 6 with conclusion given in section 7.

2. Resonator design

The re-entrant cavity resonator shown in figure 1 is designed with the following dimensions: a radius, $r_1 = 25$ mm, height, $h = 25.45$ mm, and post radius of, $r_0 = 11.25$ mm with a gap, $d = 2$ mm between the post and the cavity base. The post was rounded by a curvature with a radius, $r_b = 11.25$ mm to maximise its quality factor. Computers simulation technology (CST) Microwave Studio is used for the design and simulations [21]. To further improve the quality factor of the resonator and reduce the electric field build up at the edges and sharp corners, additional rounded corners were introduced where the top cavity wall and the post join, with a radius of $r_c = 6.75$ mm as shown in figure 1(b). Transmission-type configuration enabled by two identical straight port probes for external coupling is adopted. The probe is capacitive but deliberately positioned to where the magnetic field is high. This renders low coupling which reduces the loading effect on the resonant cavity and its Q. The used Subminiature version A (SMA) coaxial probes have a conductor diameter of 1.3 mm and penetrating length into the cavity of 2.9 mm. To achieve an insertion loss of over 20 dB the coupling was made

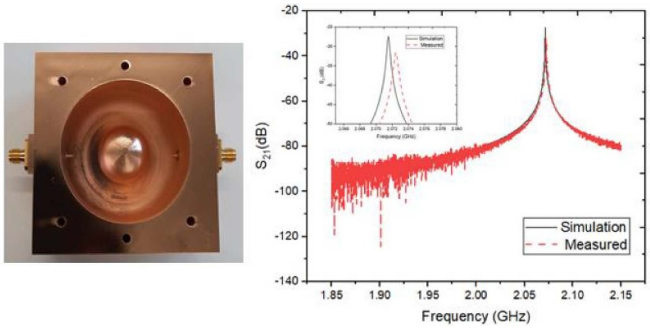

Figure 2. Photograph of the (a) 3D printed prototype and (b) S_{21} response of the measured and simulated cavity with copper base.

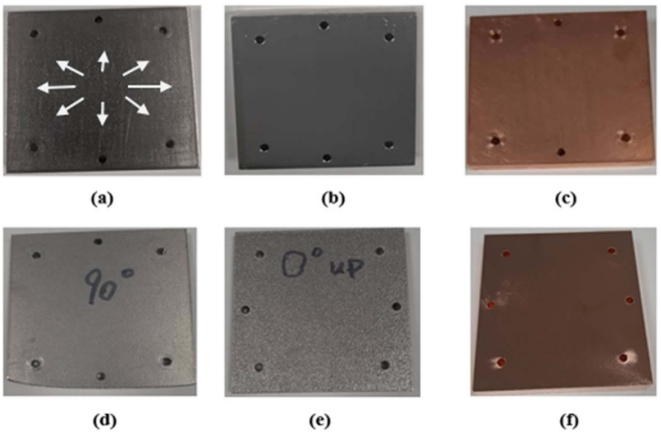

Figure 3. Photograph of the six samples. CNC machined: (a) stainless steel, (b) aluminium, (c) copper; 3D printed, (d) aluminium alloy horizontally built, (e) aluminium alloy vertically built and (f) polymer + copper plating.

weak, thereby reducing loading effect, thus external Q-factor becomes large.

The device is fabricated using SLA 3D printing using polymer and was coated with 25 μm copper as shown in the photo of the prototype in figure 2(a). The round corners introduced also help with good plating as sharp corners can be missed out during plating. The cavity is housed in a rectangular frame and is split into two parts, the top part being the main cavity and the bottom part makes the base as shown earlier in figure 1(a). The base is considered as the MUT in this case. The cavity can be assembled via the six drilled holes using 3 × 50 mm nuts and bolts, or alternatively using a clamp for easy and time-effective measurement.

3. Measurement method and samples

In material measurement using resonant techniques, the material properties are determined from the change in the frequency and the Q-factor due to material insertion at the desired resonant mode. In this measurement, as the conductivity is the only measurand, only the knowledge of the Q-factor is required. The method adopted is simple, and it has a unique advantage of not requiring samples to be cut into a precise thickness. The base (i.e. MUT) can be replaced easily. The cavity is assembled and connected to PNA network analyser (Agilent Technology E8382C) for the measurements. The network analyser is calibrated using 85052D kit. To minimize the measurement error in the high-Q resonance, a large number of sweep points (6401), over a bandwidth about five times the 3 dB bandwidth was used. An intermediate frequency is set to 1 kHz. The measured and simulated S-parameters response of the 3D printed cavity using copper material for both cavity and base is given in figure 2(b). The measured resonance frequency fr, loaded Q-factor Q_l and insertion loss IL are 2.073 GHz, 5045 and 31.35 dB while the simulation results are 2.072 GHz, 6145 and 27.75 dB using the nominal conductivity of copper, 5.8×10^7 S m^{-1}. The results show very good agreements, with a small frequency shift. There is relatively large Q-factor drop of about 15%. This can be largely attributed to the surface roughness associated with AM, which degrades the electrical conductivity of the device. In addition, the quality of the copper plating can also be a factor. This is further explained in section 4.

To validate the measurements technique, six flat samples made of aluminium, copper and stainless steel were measured. Three of the samples are made using 3D printing: one of which is made from Accura+ polymer and then coated with 25 μm copper, while the other two are metal 3D printed using aluminium alloy A20X (composed of 90.29 wt % Al and 4.07 wt % Cu) [22]. The metal 3D printed samples are built from different orientation of 0° (i.e. vertical orientation) and 90° (i.e. horizontal orientation) using SLM500HL machine from SLM solutions GmbH. The processing parameters used in the production are: 350 W laser power, at constant laser scanning speed of 1650 mm s^{-1}, 0.13 mm hatch spacing and contour of 200 W and scan speed of 800 mm s^{-1}. Both samples were polished using Sharmic vibration polishing with 3 mm ceramic particles. However, it was observed that the vertically oriented built sample is not as flat as the horizontal one. There is a little curvature in the sample. This will eventually alter the cavity volume and can affect the results of measurements. The remaining three samples are machined using CNC from copper, aluminium and stainless steel. Photographs of all the samples are given in figure 3. The direction of the surface current flow on the sample is indicated by the white arrow. Measurements of samples are taken several times to minimise random error. The average of the readings is used for the extraction of the effective conductivity. The transmission coefficient S_{21} of the measured samples is given in figure 4. The measured loaded Q-factor Q_l and the magnitude of the S_{21} are used in computing the unloaded Q- factor, Qu as follows [23]

$$Q_u = \frac{Q_l}{1 - S_{21}(f_o)}. \tag{1}$$

The results are given in table 1. There is a standard deviation of 6.74×10^{-4} and standard error of 3.01×10^{-4} from 3 dB

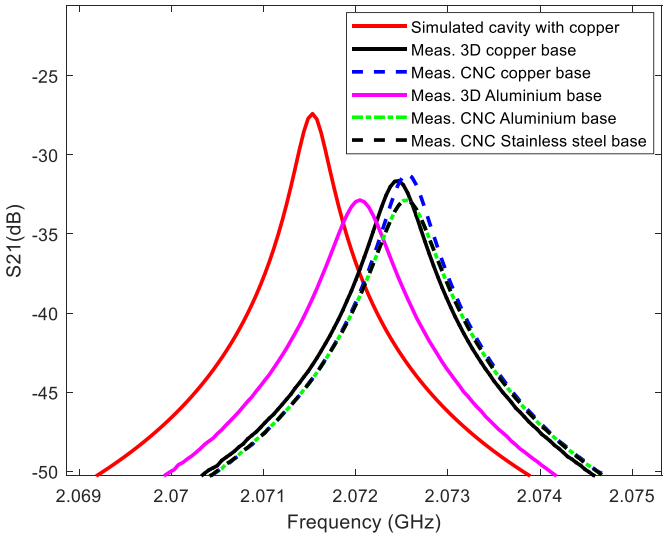

Figure 4. S_{21} response of measured materials.

Table 1. Measured loaded Q, insertion loss IL and evaluated unloaded Q using (1).

Samples	Q_l	IL (dB)	Qu
3D printed polymer with copper coating	5045	33.65	5152 ± 25
CNC copper	4936	34.01	5049 ± 15
3D printed aluminium, built horizontally (90°)	4007	35.59	4075 ± 20
3D printed aluminium, built vertically (0°)	3381	32.83	3459 ± 25
CNC aluminium	4095	35.45	4165 ± 15
CNC stainless steel	2426	40.15	2451 ± 20

bandwidth readings and the amplitude of S_{21}. This signifies good repeatability of the measurements.

4. Surface roughness

AM process tends to introduce surface features that results in or relates to microwave loss and the electrical conductivity is degraded. The knowledge of surface roughness is therefore significant in this work. This is especially so when the surface texture is in orthogonal direction to the current flow. This is also because the current flow concentrates at the surface within a few skin depths [7]. The skin depth δ is defined by [24]

$$\delta = \sqrt{\frac{1}{f\sigma\mu\pi}} \tag{2}$$

where f is the frequency, σ is conductivity, μ is permeability of the conductor.

It is noted that the surface roughness in 3D printed metal parts can be comparable with or even larger than δ. This results in increasing surface resistance and significant impact on the power loss as described [19]. The 3D-printed polymer device by SLA tends to have smoother surface. The coating helps to reduce the surface roughness further giving it advantage over AM metals. To analyse the effect of surface roughness on the effective conductivity of MUT, the surface roughness of each

Figure 5. Image of the surface measured using Alicona: (a) copper coating on 3D printed polymer sample and (b) 3D printed aluminium alloy sample.

sample was measured using Alicona microscope at three different locations. That is, the central point and two other places away from the centre. The measurement area for each location is 1×1 mm and the images of the surfaces of 3D printed: copper and aluminium alloy samples are shown in figure 5. The average height of the selected area, S_a values of the three measured points are given in table 2. From the results we can see that metal AM plates have higher surface roughness than the 3D printed polymer and the CNC plates. The S_a value of the polished vertically oriented built aluminium sample is higher than that of the polished horizontally printed sample by about 30%.

Table 2. Measured S_a value of surface roughness.

	S_a (μm) values of the three measured points
Main cavity (3D printed polymer with copper coating)	0.53, 0.54, 0.58
Base (3D printed polymer with copper coating)	0.34, 0.35. 0.38
Base (CNC copper)	0.24, 0.25, 0.27
Base (3D printed aluminium, 90°)	1.12, 1.18 1.23
Base (3D printed aluminium, 0°)	1.44, 1.57, 1.65
Base (CNC aluminium)	0.59, 0.60, 0.62
Base (CNC stainless steel)	0.50, 0.55, 0.58

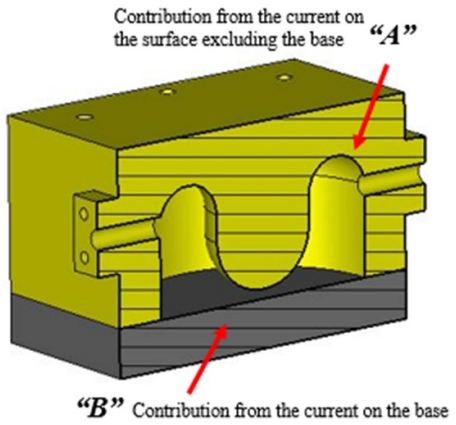

Figure 6. Illustration of contribution of current from the surface and base of the cavity: coefficient denotation.

5. Extraction method for effective conductivity

The unloaded Q is proportional to the ratio of the resonant wavelength and skin depth in any cavity structure [25]. The knowledge of Q_u can be used to evaluate the effective conductivity. This is so, for cavity with high symmetry and analytically solvable fields. However, this is not the case for the cavity used in this work. To evaluate the effective conductivity of the (MUT), an approach used in [17] was adopted. A simple analytical formula can be derived based on the knowledge of the energy stored in the volume and base of the cavity. Considering the illustration shown in figure 6, the contribution from the current on the main cavity is denoted by coefficient A, while that of the base is denoted by coefficient B. Two cases are considered: First, the main cavity and the base are of the same material (copper in this case and will also serve as the reference material). The second case is when main cavity is made of copper material and the base (MUT) is of other MUT. Based on the first case the measured unloaded Q-factor of the cavity resonator, denoted by Q_0 is related to the conductivity of the copper, σ_{CU}, given by

$$\frac{1}{Q_0} = \frac{A}{\sqrt{\sigma_{CU}}} + \frac{B}{\sqrt{\sigma_{CU}}}. \tag{3}$$

Table 3. Parameters used to extract the coefficient A and B.

Material	Conductivity (S m^{-1})	Unloaded Q-factor	Coefficient
Copper base	4.76×10^7	5863	$A = 0.901$
Aluminium base	3.56×10^7	5658	$B = 0.275$

In the second case, when the base of the cavity is replaced by the MUT. The relationship changes to

$$\frac{1}{Q_1} = \frac{A}{\sqrt{\sigma_{CU}}} + \frac{B}{\sqrt{\sigma_{MUT}}} \tag{4}$$

where Q_1 is the measured unloaded Q-factor of the cavity resonator with MUT and σ_{MUT} is the effective conductivity of the MUT. Combining (3) and (4), the measured effective conductivity of the MUT can be evaluated using the following expressions

$$\sigma_{CU} = [Q_0 (A + B)]^2 \tag{5}$$

$$\sigma_{MUT} = \frac{\sigma_{CU} B^2}{\left\{ \left[\frac{Q_0}{Q_1} (A + B) \right] - A \right\}^2}. \tag{6}$$

Since we can measure Q_0 and Q_1, we need to know the coefficient A and B in order to use (5) and (6). For this, the coefficients were determined based on simulation in CST in hypothetical experiments with given conductivity values. Two simulation models were used: one considering copper material for both the main cavity and the base, and the other considering copper material for the main cavity with an aluminium base. The nominal conductivity of these two materials taken from CST library were used in the simulation. However, following the measurements of the surface roughness of main cavity as presented earlier we have introduced surface roughness of 0.5 μm to the main part of the cavity and assume a zero roughness for the MUT as we are only concerned with the effective conductivity of the MUT. This effectively changes the conductivity of the copper material from 5.8×10^7 to 4.76×10^7 S m^{-1} at the resonant mode based on calculation from CST. Using the results of the simulations and simultaneously solving (3) and (4) gives the coefficient A and B as in table 3. It is important to note that the coefficients are not sensitive to the materials, using different nominal conductivity in generating the coefficients would give similar outcome. The uncertainty propagation of the S-parameter (S_{21}) and the measurements repeatability of cavity are used in determining the uncertainty of the measured Q-factor at 95% confidence level [26]. The uncertainty of Q-factor and that of the coefficients A and B are used to evaluate expanded uncertainty and to arrive at 95% confidence level of the measured effective conductivity.

Table 4. Measured effective conductivity.

Samples	Measured effective conductivity σ_{MUT} ($\times 10^6$ S m^{-1})	Extracted bulk conductivity using measured results ($\times 10^6$ S m^{-1})	Nominal bulk conductivity ($\times 10^6$ S m^{-1})
3D printed polymer with Cu coating	36.7 ± 0.09	39.3	58.0
CNC Cu	31.0 ± 0.08	31.9	58.0
3D printed Al alloy, (90°)	8.09 ± 0.20	9.76	29.5
3D printed Al alloy, (0°)	4.67 ± 0.12	5.64	29.5
CNC Al	9.05 ± 0.23	9.51	35.5
CNC stainless steel	1.12 ± 0.03	1.13	1.45

Table 5. Comparison with other techniques.

Type	Freq. GHz	Meas. Q-factor	Fabricatn method	Features and limitations	References
Cylindrical cavity	8.79	4045	CNC	3% accuracy on copper and brass; analytical formula	[20]
Fabry–perot open resonator	20–40	80 000	CNC	10^4–10^7 S m^{-1} demonstrated; bulky structure; a large number of resonances	[17]
Parallel plate resonator	5.3	1120	CNC	Compact resonator with relatively low Q	[19]
Re-entrant cavity	2.07	5045	3D printed coated polymer	Compact resonator with high Q; new manufacture technique	This work

6. Results discussion

The measured unloaded Q-factor (table 1) and the coefficients A and B (table 3) are utilised for computing the effective conductivity of the measured materials using (5) and (6). The results are given in table 4 along with measurement uncertainty and extracted bulk conductivity taking into account the measured surface roughness using the analytical formula in [27]. The results show that the copper coating on the 3D printed polymer and the bulk copper by CNC machining have similar conductivity values. The small difference is possibly due to sample having different conductivity, that is, copper block and the copper used in plating the 3D printed polymer. Between the 3D printed Aluminium alloy built in vertical and horizontal orientations, as expected, the one built vertically has lower conductivity compared to that of horizontally built one. This is consistent with the higher surface roughness recorded in the former. This outcome is also in conformity with the findings in [19]. For stainless steel, good agreement between the measured effective conductivity and nominal conductivity of bulk stainless steel is obtained. The effect of surface roughness is less for lower conductive materials such as the stainless steel compared to high conductive material such copper. As for the measured effective conductivity of CNC Aluminium and that of the horizontally printed sample, they have similar values. This suggests good surface conductivity of the horizontally printed aluminium-copper alloy. This also indicates how aluminium alloy A20X can be promising for utilisation in fabricating microwave devices where polishing can be applied. Generally, the results obtained are at the level of comparison with the nominal conductivity of the materials measured and reported values using other methods such as that of Aluminium alloy 8.65×10^6 S m^{-1} [18]. This has therefore validated the proposed measurement method and the evaluation formula derived and used in this work. The technique presented here offer a relatively easy and simplified measurement techniques enabled by high-Q and low cost effective conductivity measurement method compared to other method as given in table 5.

7. Conclusion

The measurement technique presented in this article uses reentrant cavity resonator for the estimation of effective conductivity of different metals under different manufacture condition or techniques. An Analytical formula for evaluating the effective conductivity based on simulations of the designed cavity and knowledge of energy stored in the cavity has been derived. The results of the measured samples show the capability of the measurement technique in distinguishing materials due to varying electrical resistances using the analytical expression. The sensitivity of the measurement setup to changes due printing orientation in AM is evident from the results of the comparison measurements. This validates the usability of the measurement technique, simple and low-cost, within acceptable systematic and random errors associated with the measurements of conductive materials for microwave applications.

Data availability statement

All data that support the findings of this study are included within the article (and any supplementary files).

Acknowledgments

A M M wishes to acknowledge Petroleum Technology Development Fund (PTDF) Nigeria for the PhD scholarship. The work is partially funded by UK EPSRC Grant EP/S013113/1.

ORCID iDs

Ali Musa Mohammed https://orcid.org/0000-0003-3121-5541
Yi Wang https://orcid.org/0000-0002-8726-402X

References

[1] Périgaud A, Bila S, Tantot O, Delhote N and Verdeyme S 2016 *3D printing of microwave passive components by different additive manufacturing technologies IEEE MTT-S Int. Microw. Workshop Series Adv. Mat. Proc.r RF THz Applic. (IMWS-AMP)* (*Chengdu, China*) (https://doi.org/10.1109/IMWS-AMP.2016.7588328)
[2] Strycharz J and Piasecki P 2018 *3D printed circular and rectangular waveguide mode converters 22nd Int. Microw. Rad. Conf. (MIKON)* (*Poznan, Poland*) (https://doi.org/10.23919/MIKON.2018.8405188)
[3] Mohammed A M, Hart A, Wood J, Wang Y and Lancaster M J 2021 3D printed re-entrant cavity resonator for complex permittivitymeasurement of crude oils *Sens. Actuators* A **317** 112477
[4] Skaik T, Salek M, Wang Y, Lancaster M, Starke T and Boettcher F 2020 *180 GHz waveguide bandpass filter fabricated by 3D printing technology 13th UK-Eur-China Workshop mm-Waves and Thz Technol. (UCMMT)* (*Tianjin, China*) (https://doi.org/10.1109/UCMMT49983.2020.9296044)
[5] Timbie P T, Grad J, Weide D, Maffei B and Pisano G 2011 *Stereolithographed Mm-wave corrugated horn antennas Int. Conf. Infrared, mm THz Waves* (*Houston, TX, USA*) (https://doi.org/10.1109/irmmw-THz.2011.6104833)
[6] Hernandez A, Martin E, Margineda J and Zamarro J M 1986 Resonant cavities for measuring the surface resistance of metals at X-band frequencies *J. Phys. E: Sci. Instrum.* **19** 222–5
[7] Maxwell E 1947 Conductivity of metallic surfaces at microwave frequencies *J. Phys. D: Appl. Phys.* **18** 628–38
[8] Beck A and Dawson R 1950 Conductivity measurements at microwave frequencies *Proc. IRE* **33** 1181–9
[9] Coué J E, Chausse H and Robert F B 1994 Conductivity and mobility contactless measurements of semiconducting layers by microwave absorption at 35 Ghz *J. Phys.* III **4** 707–18
[10] Chao S-H 1985 Measurement of microwave conductivity and dielectric consatant by the cavity pertubation method and thier errors *IEEE Trans. Microw. Theory Tech.* **33** 519–26
[11] Nakayama A, Terashi Y, Uchimura H and Fukuura A 2002 Conductivity measurements at the interface between the sintered conductor and dielectric substrate at microwave frequencies *IEEE Trans. Microw. Theory Tech.* **50** 1665–74
[12] Krupka J 2006 Frequency domain complex permittivity measurements at microwave frequencies *Meas. Sci. Technol.* **17** R55–R70
[13] Gregory A P and Clarke R N 2006 A review of RF and microwave techniques for dielectric measurements on polar liquids *IEEE Trans. Dielectr. Electr. Insul.* **13** 727–43
[14] Rmili H, Miane J-L, Olinga T E and Zangar H 2005 Microwave conductivity measurements of high conductive polyaniline films *J. Phys. D: Appl. Phys.* **29** 65–72
[15] Ritza E and Dressel M 2008 Analysis of broadband microwave conductivity and permittivity measurements of semiconducting materials *J. Appl. Phys.* **103** 1–8
[16] Bobowski J S and Clements A P 2017 Permittivity and conductivity measured using a novel toroidal split-ring resonator *IEEE Trans. Microw. Theory Tech.* **65** 2132–8
[17] Cuper J, Salski B, Karpisz T, Pacewicz A and Kopyt P 2020 *Conductivity measurement in mm-wave band with a Fabry–Perot open resonator IEEE/MTT-S Int Microw. Symp. (IMS)* (*Los Angeles, CA, USA*) (https://doi.org/10.1109/IMS30576.2020.9224069)
[18] Edwards R G, Norton C M, Campbell J E and Schurig D 2021 Effective conductivity of additive-manufactured metals for microwave feed components *IEEE Access* **9** 59979–86
[19] Gumbleton R, Cuenca J A, Hefford S, Nai K and Porch A 2021 Measurement technique for microwave surface resistance of additive manufactured metals *IEEE Trans. Microw. Theory Tech.* **69** 189–97
[20] Barroso J J, Castro P J and Neto J P L 2003 Electrical conductivity measurement through the loaded q factor of a resonant cavity *Int. J. Infrared Millim. Waves* **24** 79–86
[21] Computer Simulated Technology Microwave Studio 2020 *Uniiversity of Birmigham Software centre* (available at: www.cst.com/) (Accessed 1 February 2020)
[22] Bale P 2011 *Feeding Properties of The Highly Grain Refined A20x Alloy* (Birmingham: University of Birmingham) (available at: https://etheses.bham.ac.uk/id/eprint/3327/1/Bale_12_MRes.pdf)
[23] Lancaster M J 1997 *Passive Microwave Device Applictaions of High Temperature Supercoductors* (Cambridge: Cambridge University Press) pp 67–125
[24] Rizzi P A 2002 *Microwave Engineering Passive Circuit* 2nd edn (NJ: Prentice Hall)
[25] Kim H S 2011 Electromagnetic wave in cavity design *Behaviour of Electromagnetic Waves in Different Media and Structures* (Rijeka: InTech) pp 80–83
[26] Bell S 2001 *A Beginner's Guide to Uncertainty of Measurement* (Middlesex: National Physics Laboratory)
[27] Hammerstad E and Jensen O 1980 *Accurate models for microstrip computer-aided design IEEE MTT-S Int. Microw. Symp. Dig.* (*Washington, DC, USA*) (https://doi.org/10.1109/MWSYM.1980.1124303)